Wave-Induced Sediment Transport and Sandbar Migration

Fernanda Hoefel[1] and Steve Elgar[2]

Onshore sediment transport and sandbar migration are important to the morphological evolution of beaches but are not well understood. Here, a model that accounts for fluid accelerations in waves predicts the onshore sandbar migration observed on an ocean beach. In both the observations and the model, the location of the maximum acceleration-induced transport moves shoreward with the sandbar, resulting in feedback between waves and morphology that drives the bar shoreward until conditions change. A model that combines the effects of transport by waves and mean currents simulated both onshore and offshore bar migration observed over a 45-day period.

Surf zone sandbars protect beaches from wave attack and are a primary expression of cross-shore sediment transport. During storms, intense wave breaking on the bar crest drives strong offshore-directed currents ("undertow") that carry sediment seaward, resulting in offshore sandbar migration (*1, 2*) (Fig. 1A). If the beach morphology is in equilibrium, the offshore migration is balanced by slower onshore transport between storms (*3, 4*). However, the causes of shoreward sediment transport and sandbar migration are not known, and thus models for beach evolution are not accurate (*1, 2, 5, 6*).

As waves enter shallow water, their shapes evolve from sinusoidal to peaky, with sharp wave crests separated by broad, flat wave troughs. It has been hypothesized that the larger onshore velocities under the peaked wave crests transport more sediment than the offshore velocities under the troughs (*7, 8*). However, models that account for the onshore-skewed velocities do not accurately predict onshore bar migration observed near the shoreline and in the surf zone (*1, 2, 5, 6*), although skewed velocities may be important outside the surf zone (*9*). As waves continue to shoal and break, they evolve from profiles with sharp peaks to asymmetrical, pitched-forward shapes with steep front faces. Water rapidly accelerates under the steep wave front, producing high onshore velocities, followed by smaller decelerations under the gently sloping rear of the wave (Fig. 1B) (*10, 11*). Large accelerations generate strong horizontal pressure gradients that act on the sediment (*12–14*). Although the precise mechanisms are not fully understood, it has been hypothesized that if accelerations increase the amount of sediment in motion (*10, 12, 15, 16*), there will be more shoreward than seaward transport under pitched-forward waves.

A surrogate for the effects of acceleration in pitched-forward waves is a dimensional form of acceleration skewness (*12*) (i.e., the difference in the magnitudes of accelerations under the front and rear wave faces), $a_{\mathrm{spike}} = \langle a^3 \rangle / \langle a^2 \rangle$, where a is the time series of acceleration and angle brackets denote averaging. Discrete-particle computer simulations of bedload transport driven by asymmetrical waves characteristic of surf zones indicate that sediment flux is proportional to a_{spike} once a threshold for sediment motion is exceeded (*12*). Unlike the monochromatic waves used in the numerical simulations, accelerations in random waves in a natural surf zone can be skewed either positively (onshore) or negatively (offshore). Thus, the expression for cross-shore (x) acceleration-driven bedload sediment transport $Q_{\mathrm{acc}}(x)$ suggested by the numerical simulations is extended to account for random waves by including a term that depends on the sign (i.e., the direction) of a_{spike}, yielding

$$Q_{\mathrm{acc}}(x) = \begin{cases} K_{\mathrm{a}}(a_{\mathrm{spike}} - \mathrm{sgn}[a_{\mathrm{spike}}]a_{\mathrm{crit}}) & \text{for } |a_{\mathrm{spike}}| \geq a_{\mathrm{crit}} \\ 0 & \text{for } |a_{\mathrm{spike}}| < a_{\mathrm{crit}} \end{cases} \quad (1)$$

where K_{a} is a constant, sgn[ ] is the sign of the argument, and a_{crit} is a threshold that must be exceeded for initiation of transport.

[1]Massachusetts Institute of Technology/Woods Hole Oceanographic Institution (WHOI) Joint Program in Oceanography, WHOI, Mail Stop 09, Woods Hole, MA 02543, USA. [2]WHOI, Mail Stop 11, Woods Hole, MA 02543, USA. E-mail: fhoefel@whoi.edu, elgar@whoi.edu

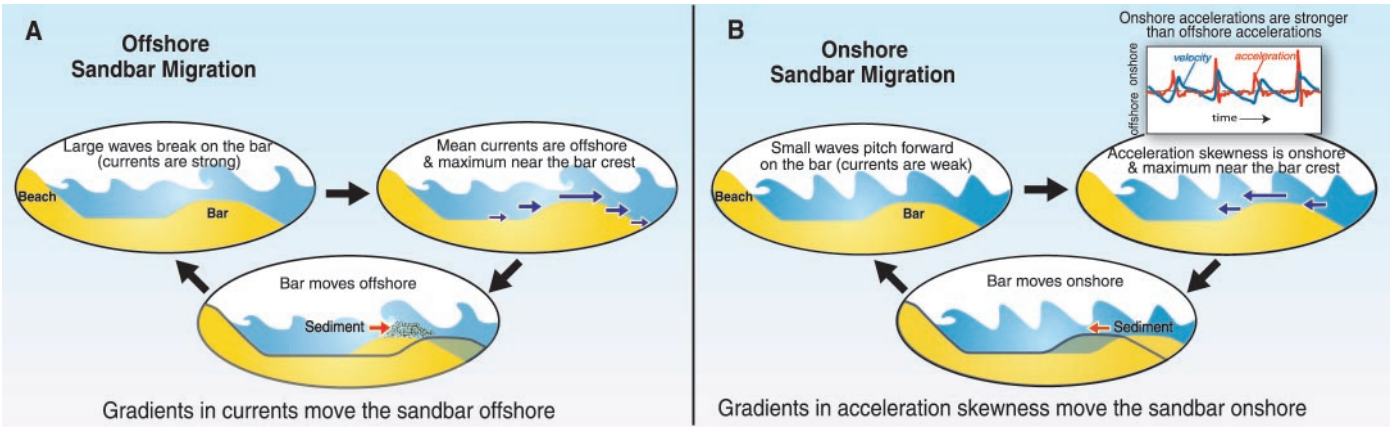

Fig. 1. Schematic of the feedbacks that drive sandbar migration. (**A**) Large waves in storms break on the sandbar, driving a strong offshore-directed current (undertow) that is maximum just onshore of the bar crest (*2*). The cross-shore changes (gradients) in the strength of the undertow result in erosion onshore, and deposition offshore of the sandbar crest, and thus offshore bar migration. The location of wave breaking and the maximum of the undertow move offshore with the sandbar, resulting in feedback between waves, currents, and morphological change that drives the bar offshore until conditions change. (**B**) Small waves do not break on the bar, but develop pitched-forward shapes. Water is rapidly accelerated toward the shore under the steep front face of the waves and decelerates slowly under the gently sloping rear faces. Thus, the time series of acceleration is skewed, with larger onshore than offshore values (rectangular panel). The cross-shore gradients in acceleration skewness (maximum on the bar crest) result in erosion offshore, and deposition onshore of the bar crest, and thus onshore bar migration. The location of the peak in acceleration skewness moves onshore with the sandbar, resulting in feedback between waves, currents, and morphological change that drives the bar onshore until conditions change.

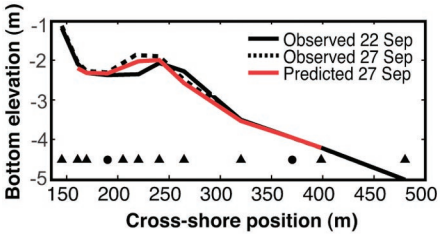

Fig. 2. Observed and predicted cross-shore bottom elevation profiles. Elevation of the seafloor relative to mean sea level observed on 22 September 1994, 1900 hours EST (black solid curve), observed on 27 September 1994, 1900 hours (black dashed curve), and predicted by the acceleration-based transport model (red curve) versus cross-shore position. The energetics transport model [using parameters in (*2*)] without acceleration predicts no change in the sea floor (*2*). Cross-shore locations of colocated pressure sensors, current meters, and altimeters are indicated by triangles, and locations of colocated pressure sensors and current meters by circles. Observed near-bottom velocities (sampled at 2 Hz) were low-pass filtered (cutoff frequency = 0.5 Hz) and differentiated in time to obtain near-bottom acceleration time series. Sediment transport fluxes for the model predictions were computed from 3-hour averages of observed near-bottom velocity and acceleration statistics, and integrated in time with a 3-hour time step (Eq. 2) to compute predicted bottom elevation changes. Mean sediment grain sizes ranged from 0.30 mm at the shoreline to 0.15 mm in water depth of 5 m (*2*).

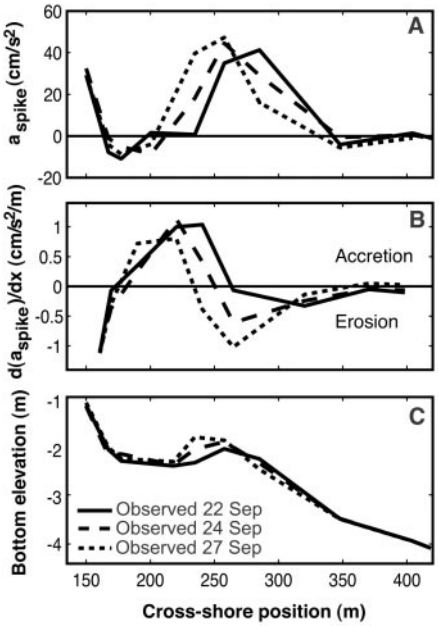

Fig. 3. Acceleration skewness and bottom elevation profiles during an onshore sandbar migration event. (**A**) Observed acceleration skewness (a_{spike}), (**B**) cross-shore gradient of acceleration skewness, and (**C**) sea-floor elevation relative to mean sea level versus cross-shore position. The solid curves are observations from 22 September 1994, 1900 to 2200 hours; dashed curves are 24 September 1994, 1300 to 1600 hours; and dotted curves are 27 September 1994, 1900 to 2200 hours.

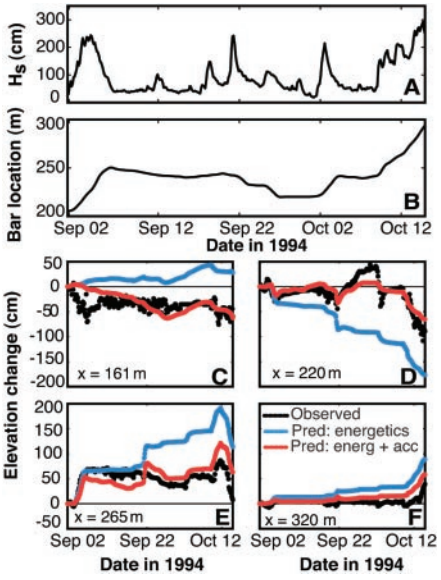

Fig. 4. Observed wave height, cross-shore sandbar crest position, and observed and predicted bottom elevation changes at four cross-shore locations between 1 September 1994, 1900 hours and 15 October 1994, 2200 hours. (**A**) Significant wave height (four times the standard deviation of 3-hour-long records of sea surface elevation fluctuations in the frequency bands between 0.01 and 0.3 Hz) observed in 5 m water depth and (**B**) cross-shore position of the sandbar crest versus time. The bar crest position was estimated from spatially dense surveys conducted with an amphibious vehicle approximately biweekly, combined with 3-hour estimates of sea-floor elevation from altimeter measurements (*2*) (Fig. 1). The shoreline fluctuated (owing to a 1-m tide range) about cross-shore location x = 125 m. Observed (black circles) and predicted (blue curve for energetics model, red curve for combined energetics and acceleration model) cumulative change in sea-floor elevation at cross-shore locations (**C**) x = 161 m, (**D**) x = 220 m, (**E**) x = 265 m, and (**F**) x = 320 m. Parameters in the energetics models are the same as those in (*2*).

By comparing model predictions with observations, the optimal values of $K_a = 1.40 \times 10^{-4}$ m s and of $a_{crit} = 0.20$ m s^{-2} were determined. These parameter values are within a factor of 5 of those suggested by the highly idealized discrete-particle numerical simulations (*12*) ($K_a = 0.26 \times 10^{-4}$ m s, $a_{crit} = 1.00$ m s^{-2}). Differences may be attributable to random waves, a distribution of sediment grain sizes and shapes, and breaking-induced turbulence in the ocean. If it is assumed that gradients in alongshore transport are negligible, mass conservation in the cross-shore direction yields

$$\frac{dh}{dt} = \frac{1}{\mu}\frac{dQ_{acc}(x)}{dx} \qquad (2)$$

where dh/dt is the change in bed elevation h with time t and $\mu = 0.7$ is a sediment packing factor. Extensions to Eq. 2 to account for alongshore changes are straightforward, but not necessary for the small alongshore gradients in transport inferred for the observations discussed here (*2*).

To test the hypothesis that the cross-shore distribution of near-bottom accelerations results in overall onshore sediment transport and sandbar migration when mean currents are weak, we compared morphological change predicted by the acceleration-based model (Eqs. 1 and 2) with observations made along a cross-shore transect extending about 400 m from the shoreline to 5 m water depth on the North Carolina coast (*2, 17*). The model was initialized (t = 0) with observed bathymetry and driven with accelerations observed with near-bottom–mounted current meters (Fig. 2). During a 5-day period with approximately 75-cm-high waves and cross-shore mean currents less than 30 cm s^{-1}, the observed onshore sandbar migration of about 30 m was predicted accurately (Fig. 2). A widely used energetics sediment transport model (*1, 2, 7, 8, 18*) that accounts for transport both by velocity skewness (but not acceleration) and by mean currents predicted no change in the cross-shore depth profile and thus failed to predict the observed sandbar migration (*2*).

During the onshore sandbar migration event, acceleration skewness (a_{spike}) increased from small values offshore to a maximum near the bar crest and then decreased toward the shoreline (Fig. 3, A and C), producing cross-shore gradients in transport that are consistent with erosion offshore and accretion onshore of the bar crest (Fig. 3, B and C). The peak in acceleration skewness moved shoreward with the bar crest (Fig. 3), resulting in feedback between wave evolution and bathymetry that promoted continued onshore sediment transport and bar movement until conditions changed (Fig. 1B). Feedback also occurs between wave-breaking–induced offshore-directed mean currents (maximum just onshore of the bar crest) and morphology that results in offshore bar migration during storms (*1, 2*) (Fig. 1A).

Inclusion of the effects of skewed accelerations (Eq. 1) in the energetics-based sediment transport model (*1, 2, 7, 8, 18*) resulted in improved predictive skill, both when mean cross-shore currents were weak (Fig. 2) and during storms when mean currents were strong (Fig. 4). During a 45-day observational period, the bar crest migrated offshore about 130 m during storms and onshore about 40 m when waves and mean flows were small (Fig. 4B), resulting in a net offshore migration of 90 m. Although

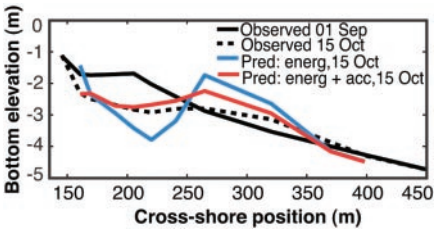

Fig. 5. Observed and predicted cross-shore bottom elevation profiles spanning a 45-day period. Sea-floor elevation relative to mean sea level observed 1 September 1994, 1900 hours (solid black curve), observed 15 October 1994, 2200 hours (dashed black), and predicted for 15 October 1994, 2200 hours by the energetics (blue) and energetics plus acceleration (red) models versus cross-shore position.

energetics models without acceleration-based transport predicted the offshore migration (*1, 2*), they had limited skill predicting the total change to the beach over 45 days because they failed to predict onshore migration between storms (*2*). The energetics model that was extended to include acceleration better predicted the change in the sea-floor both onshore and offshore of the bar crest (Fig. 4), and the overall evolution of the cross-shore depth profile (Fig. 5).

References and Notes

1. E. Thornton, R. Humiston, W. Birkemeier, *J. Geophys. Res.* **101**, 12097 (1996).
2. E. Gallagher, S. Elgar, R. Guza, *J. Geophys. Res.* **103**, 3203 (1998).
3. D. Aubrey, *J. Geophys. Res.* **84**, 6347 (1979).
4. L. Wright, A. Short, *Mar. Geol.* **56**, 93 (1984).
5. J. Roelvink, M. Stive, *J. Geophys. Res.* **94**, 4185 (1989).
6. L. Wright, J. Boon, S. Kim, J. List, *Mar. Geol.* **96**, 19 (1991).
7. A. Bowen, in *The Coastline of Canada*, S. McCann, Ed. (Geol. Surv. Canada Pap. 10-80, Ottawa, Canada, 1980), pp. 1–11.
8. J. Bailard, *J. Geophys. Res.* **86**, 10938 (1981).
9. J. Trowbridge, D. Young, *J. Geophys. Res.* **94**, 10971 (1989).
10. S. Elgar, E. Gallagher, R. Guza, *J. Geophys. Res.* **106**, 11623 (2001).
11. S. Elgar, R. Guza, M. Freilich, *J. Geophys. Res.* **93**, 9261 (1988).
12. T. G. Drake, J. Calantoni, *J. Geophys. Res.* **106**, 19859 (2001).
13. O. Madsen, in *Proc. 14th Int. Conf. Coastal Eng.*, Copenhagen, Denmark (American Society of Civil Engineers, Reston, VA, 1974), p. 776–794.
14. P. Nielsen, *Coastal Eng.* **45**, 53 (2002).
15. R. Hallermeier, *Cont. Shelf Res.* **1**, 159 (1982).
16. D. Hanes, D. Huntley, *Cont. Shelf Res.* **6**, 585 (1986).
17. E. Gallagher, S. Elgar, E. Thornton, *Nature* **394**, 165 (1998).
18. R. Bagnold, *U.S. Geol. Surv. Prof. Pap. 422-I* (1966).
19. Support was provided by the Army Research Office, the Office of Naval Research, NSF, and a fellowship from Conselho Nacional de Desenvolvimento Científico e Tecnológico (CNPq), Brazil. E. Gallagher, R. Guza, T. Herbers, and B. Raubenheimer made valuable comments and helped obtain the field observations. The staff of the Field Research Facility and the Center for Coastal Studies provided excellent logistical support during arduous field conditions.

12 December 2002; accepted 12 February 2003

Hexapod Origins: Monophyletic or Paraphyletic?

Francesco Nardi,[1]* Giacomo Spinsanti,[1] Jeffrey L. Boore,[2] Antonio Carapelli,[1] Romano Dallai,[1] Francesco Frati[1]

Recent morphological and molecular evidence has changed interpretations of arthropod phylogeny and evolution. Here we compare complete mitochondrial genomes to show that Collembola, a wingless group traditionally considered as basal to all insects, appears instead to constitute a separate evolutionary lineage that branched much earlier than the separation of many crustaceans and insects and independently adapted to life on land. Therefore, the taxon Hexapoda, as commonly defined to include all six-legged arthropods, is not monophyletic.

The phylum Arthropoda comprises the major groups Hexapoda (insects and presumed allies), Myriapoda (e.g., centipedes and millipedes), Chelicerata (e.g., spiders and horseshoe crabs), and Crustacea (e.g., crabs and lobsters). Many studies have attempted to reconstruct the evolutionary relationships among arthropods using various approaches such as paleontology (*1*), comparative morphology (*2*), comparative developmental biology (*3*, *4*), and molecular phylogenetics (*5*, *6*).

It has long been held that hexapods (*7*) constitute a monophyletic taxon (*8*, *9*) and that their closest relatives are to be found in myriapods (*10*). More recently, molecular and developmental studies have rejected this relationship (*3–5*, *11*, *12*) in favor of a closer affinity between Hexapoda and Crustacea (Pancrustacea or Tetraconata). In this context, special attention must be given to the apterygotes (springtails, silverfish, and their allies), the wingless hexapods thought to branch at the base of Hexapoda. The phylogenetic position of these groups is still unclear (*13–16*), casting doubt even on the monophyly of the Hexapoda (*17*).

A potentially powerful technique for resolving deep relationships is to compare whole mitochondrial genomes (*5*, *17*, *18*). Phylogenetic analysis of the only complete mitochondrial sequence available for an apterygotan species (*17*) suggested the possibility that Collembola might not be included within Hexapoda, contrasting with the classic view of a monophyletic taxon that includes all six-legged arthropods. Collembola have been clustered within crustaceans in other molecular and/or combined data sets (*15*, *16*), but the possible paraphyly of Hexapoda has not been given specific attention and the deserved consideration. We have now sequenced the complete mitochondrial genomes of two additional species (*19*) specifically chosen to address this problem: *Tricholepidion gertschi*, representing one of the most basal lineages of the Insecta (Zygentoma), and *Gomphiocephalus hodgsoni*, another collembolan, to test support for the two competing hypotheses of a monophyletic versus paraphyletic Hexapoda.

An initial phylogenetic analysis performed on the 35-taxon data set (*19*) produced the tree shown in Fig. 1. The tree has high support at most nodes, with support decreasing toward deeper relationships. This analysis strongly supports the Pancrustacea hypothesis, with the exception of the position of *Apis* and *Heterodoxus*. *T. gertschi* is basal to all the pterygotan insects, supporting the monophyly of the Insecta. The four crustacean sequences are divided into two well-defined groups (representing Malacostraca and Branchiopoda), but their reciprocal relationships and position relative to the Insecta are not resolved. The Crustacea + Insecta node is well supported, and it excludes the two collembolans, which cluster together as the basal lineage of the Pancrustacea. A second group unites the Chelicerata + Myriapoda [as in (*20*)] but also includes the insects *Apis* and *Heterodoxus*, presumably as an artefact.

Although this tree shows many interesting outcomes, it also contains some evidently untenable relationships, which nevertheless have strong statistical support. This indicates the presence of anomalies in the evolution of these sequences that introduce strong systematic errors in the analysis. The most likely factors that can cause these anomalies are unequal base composition [which can bias amino acid composition (*21*)] and uneven rates of evolution among different lineages. This problem might be especially acute, because some taxa share an extremely high AT bias—*Apis* (84.8%), *Rhipicephalus* (78.0%), and *Heterodoxus* (79.3%)—and different rates of evolution,

[1]Department of Evolutionary Biology, University of Siena, via Aldo Moro 2, 53100 Siena, Italy. [2]U.S. Department of Energy Joint Genome Institute and Lawrence Berkeley National Laboratory, 2800 Mitchell Drive, Walnut Creek, CA 94598, USA.

*To whom correspondence should be addressed. E-mail: nardifra@unisi.it

the winged insects. The authors took each of the 13 protein-coding genes typically found in animal mitochondrial genomes and aligned them with those of other arthropods whose mitochondrial genomes have been completely sequenced. To root their phylogenetic trees, they also included mitochondrial genome sequence data for several out-groups, making a total of 35 taxa subjected to phylogenetic analysis.

Their initial phylogenetic analysis is interesting because it reveals the effects of systematic biases in sequence data on the recovery of a believable tree of relationships. The most spectacularly unbelievable result of this intentionally naïve analysis is a strongly supported grouping of two insects (honeybee and louse) with two ticks (chelicerates). Inspection of the data reveals at least part of the reason for this obvious anomaly—a convergent high A + T base composition in the mitochondrial genome sequences. Another potential source of systematic bias is the lineage-specific differences in rates of evolution—rapidly evolving lines may group artifactually, the so-called "long branches attract" phenomenon (*5*).

Nardi and colleagues mitigate the effects of these biases by winnowing their data to remove taxa that are not compatible in base composition and relative rates of evolution with the taxa (collembola and silverfish) that they deem crucial for testing the hypothesis of hexapod monophyly. They lose more than half their taxa in this exercise, leaving 15, but they remove obvious bias from the remaining data. Now they find strong evidence linking hexapods with crustaceans. This in itself is another point of major contention among those studying arthropod phylogenetics. For many years, Myriapods have been considered the closest relatives of hexapods. But, more recently, new data from molecular phylogenetics and developmental biology support a close relationship between hexapods and crustaceans. This grouping has had its proponents in the past: A hundred years ago a former director of my institution—then known as the British Museum (Natural History)—placed the hexapods and crustaceans together (*6*). The findings of Nardi *et al*. and other recent work force a careful look at data from all sources (*7*).

The final analyses of Nardi and co-workers appear to be very conservative and strongly support the separation of the collembolans from the insects by the two remaining species of crustaceans (see the figure). Many arthropod experts will not be entirely convinced by these data. Systematics is a very contentious field, so we can count on criticisms about the small number of species, the single data type, and the method of analysis. But at the very least, these data will spur both the collection of more sequence data from more taxa and also the extension and reevaluation of morphological work. Whatever the outcome, we will have a more solid understanding of how six-legged animals colonized and then took over the terrestrial world.

References

1. R. A. Fortey, R. H. Thomas, Eds., *Arthropod Relationships* (Chapman and Hall, London, 1997).
2. F. Nardi *et al.*, *Science* **299**, 1887 (2003).
3. P. E. S. Whalley, E. A. Jarzembowski, *Nature* **291**, 317 (1981).
4. F. Haas *et al.*, *Organisms Divers. Evol.* **3**, 39 (2003).
5. J. Felsenstein, *Syst. Zool.* **27**, 401 (1978).
6. E. R. Lankester, *Q. J. Microsc. Sci.* **47**, 523 (1904).
7. K. D. Klass, N. P. Kristensen, *Ann. Soc. Entomol. Fr.* **37**, 265 (2001).

GEOPHYSICS

Sandbars in Motion

Marcel J. F. Stive and Ad J. H. M. Reniers

Below the apparently chaotic sea surface of surf zones, complex sandbar patterns with intricate structure are frequently observed (see the left panel of the figure). Increasing ability to monitor these morphodynamic patterns has so far met with modest success in explaining their complexity. Near-shore morphodynamic models are therefore restricted to short time scales (a few weeks or less) and energetic storm conditions. On page 1885 of this issue, Hoefel and Elgar (*1*) introduce a new transport mechanism based on flow acceleration within the waves that may help to extend the prediction time scales of these models.

Interest in sandbar patterns first arose when it became clear that they play a role in predicting the likelihood of rip currents, which form a hazard to swimmers. In a pioneering study, Wright and Short (*2*) examined near-shore variability on Australian beaches and introduced a classification of observed beach states. Lippmann and Holman (*3*) extended this classification on the basis of their examination of day-to-day variability of near-shore morphology at Duck, North Carolina, with video techniques (see the figure). These and other observations have shown that sandbar dynamics are often complex, sometimes showing spatial or temporal periodicity along the shore and at other times displaying more chaotic behavior (*3*).

Surf zone processes are highly nonlinear, creating nontrivial responses to input forcing. To understand and predict sandbar behavior, it is crucial to establish whether we are dealing with a deterministic forced response, a deterministic chaotic response, or a stochastic chaotic response—and, if so, when. Offshore bar migration, which occurs under highly energetic conditions, is an example of a deterministically forced response, where perturbations are suppressed and are advected offshore by negative feedback between water motion and bed motion (*4, 5*).

In the case of chaotic behavior, positive feedbacks promote the selective growth of small perturbations, leading to self-organization. Whether the chaotic response is deterministic or stochastic depends on how long the forcing conditions prevail. A simple example of deterministic chaos is an undulating coastline exposed to dominant incident wave angles greater than 45°, causing initially unlimited growth of coastline perturbations (*6*).

More complex deterministic chaos in surf zone topography structures may be understood through linear and nonlinear stability analyses. An initial equilibrium state is subjected to small perturbations in the forcing and/or water depth, and the fastest growing modes are identified as the most likely structures to appear (*7, 8*). An alternative approach is based on cellular automata (*9*), which can mimic both deterministic and stochastic chaotic behavior in beach cusps (*10*).

However, in the case of beach cusps, similar results can also be obtained based on deterministic forcing by phase-locked edge waves superimposed on the incident waves (*11*). Also, data analyses examining the measure of chaotic behavior in observed near-shore response (*12*) have not been conclusive (*13*). Because all these approaches predict morphodynamic responses that have frequently been observed in the field, we conclude that the three response mechanisms probably all occur and might even coexist. Identifying the range of time and spatial scales for the deterministic forcing of near-shore morphodynamic response remains an intriguing prediction problem.

M. J. F. Stive is at the Faculty of Civil Engineering and Geosciences, Delft University of Technology, 2600 GA Delft, Netherlands. E-mail: m.j.f.stive@ct.tudelft.nl A. J. H. M. Reniers is at the Naval Postgraduate School, Monterey, CA 93943, USA. E-mail: areniers@nps.navy.mil

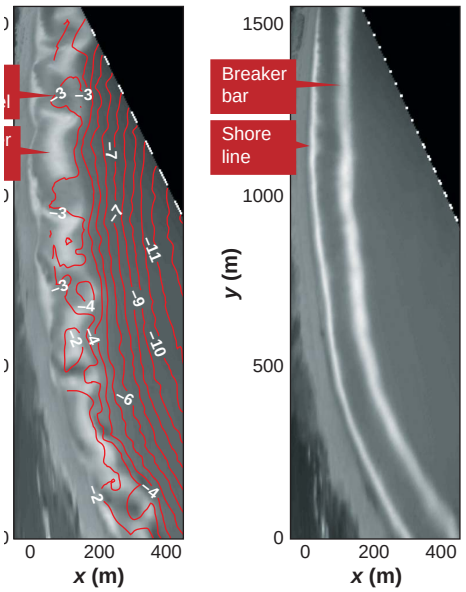

Breaking waves. ARGUS stations (Coastal Imaging Lab, Oregon State University) overlooking part of a beach are used to obtain photographic images of incident wave breaking. Waves prefer to break over shallow bars, where the foam of the breaking waves shows up as an area of high light intensity. By averaging over a large number of images (equivalent to a photographic time exposure), a stable estimate of light intensity is obtained (*3*). The sharp contrast in light intensity between areas of breaking and nonbreaking waves reflects the position of shallow bar areas and deeper channels and troughs. (**Left**) A time exposure of Palm Beach, Australia, with superposed bottom contours (sea-floor depth in meters with respect to mean sea level) displays a complex pattern of shallow shoals (light areas) cut by deep rip channels (dark areas). The beach is located on the left. (**Right**) A time exposure at the same beach shows intense wave breaking on a linear bar and additional breaking at the shoreline.

Highly energetic wave conditions often destroy the complex three-dimensional surf zone structures (*3*), resulting in one or more uniform linear bars along the shore (see the right panel of the figure). Although it has not been shown by any of the modeling efforts described above, this is generally considered to be a forced response. What has been shown to be a forced response is the offshore migration of the linear bars when energetic conditions continue to prevail (*4, 5*). The sediment transport formulation in all prevailing models is based on near-bed velocities derived from experiment or theory (*14, 15*). Applying a similar approach during mild wave conditions typically results in incorrect onshore motion of the bar, or even the failure of onshore motion (*16*).

Hoefel and Elgar (*1*) now show that this onshore motion can also be predicted with a deterministically forced sediment transport model, provided that the sediment transport induced by flow acceleration within the waves is included. They extend a formulation by Drake and Calantoni (*17*) based on detailed numerical modeling of particle-fluid interactions in a sediment layer to the case of random waves, appropriate for field conditions. Hoefel and Elgar (*1*) demonstrate improved prediction of near-shore bar motion over a 45-day period. This implies a substantial extension of prediction horizons of deterministic forced models.

The introduction of wave acceleration or, more generally, temporal and spatial pressure gradients (*17–19*) is an important paradigm shift in describing and modeling sediment transport. Prevailing concepts are based on shear stress or work exerted by fluid velocities. Introducing pressure gradients will give a new boost to understanding sediment transport near the shore.

Do these findings imply that surf zone bar structures are deterministically forced and thus deterministically predictable? The answer has to be negative. Many studies of seabed and land geomorphology (*9, 20*) show that self-organization processes lead to emergent properties, which cannot be predicted from the physics of fundamental particles. What is shown, though, is that reductionist studies can still yield new insights and that the fashionable self-organizational research approach is not the only route to increased understanding.

What hampers reductionist research progress is the enormous effort required to unravel physical processes from first principles. Hoefel and Elgar show that it pays off. Their study is a first step toward an operational new sediment transport approach. Developing this model further will require new physical insights and capabilities for modeling such phenomena as nonlinear wave kinematics in the surf zone.

References

1. F. Hoefel, S. Elgar, *Science* **299**, 1885 (2003).
2. L. D. Wright, A. D. Short, *Mar. Geol.* **56**, 93 (1984).
3. T. C. Lippmann, R. A. Holman, *J. Geophys. Res.* **97**, 11575 (1990).
4. J. A. Roelvink, M. J. F. Stive, *J. Geophys. Res.* **94**, 4785 (1989).
5. E. B. Thornton, R. Humiston, W. Birkemeier, *J. Geophys. Res.* **101**, 12097 (1996).
6. A. Ashton, A. B. Murray, O. Arnault, *Nature* **414**, 296 (2001).
7. R. Deigaard, N. Drønen, J. Fredsøe, J. Jensen, M. Jørgensen, *Coastal Eng.* **36**, 171 (1999).
8. A. Falques, G. Coco, D. A. Huntley, *J. Geophys. Res.* **105**, 24701 (2000).
9. B. T. Werner, T. Fink, *Science* **260**, 968 (1993).
10. G. Coco, D. A. Huntley, T. J. O'Hare, *J. Geophys. Res.* **105**, 21991 (2000).
11. R. T. Guza, D. L. Inmann, *J. Geophys. Res.* **80**, 2997 (1975).
12. H. N. Southgate, I. Moller, *J. Geophys. Res.* **105**, 11489 (2000).
13. S. Elgar, *J. Geophys. Res.* **106**, 4625 (2001).
14. A. J. Bowen, in *The Coastline of Canada*, S. McCann, Ed., Paper 10-80 (Geol. Surv. Canada, Ottawa, 1980), pp. 1–11.
15. J. A. Bailard, *J. Geophys. Res.* **86**, 10938 (1981).
16. E. Gallagher, S. Elgar, R. T. Guza, *J. Geophys. Res.* **103**, 3203 (1998).
17. T. G. Drake, J. Calantoni, *J. Geophys. Res.* **106**, 19859 (2001).
18. S. Elgar, R. T. Guza, M. Freilich, *J. Geophys. Res.* **93**, 9261 (1988).
19. S. Elgar, E. Gallagher, R.T. Guza, *J. Geophys. Res.* **106**, 11623 (2001).
20. M. A. Kessler, B. T. Werner, *Science* **299**, 380 (2003).

NEUROSCIENCE

Gambling on Dopamine

Peter Shizgal and Andreas Arvanitogiannis

With bated breath, a player at a roulette table stares intently at the spinning wheel. As the ball comes to rest in one of the numbered slots, a smile crosses the gambler's face. This success strengthens his misguided belief in his ability to overcome the house advantage, and he prepares to wager again. The gambler's ability to detect the slot where the ball has settled depends on point-to-point connections between nerve cells at multiple levels of the visual system. The accompanying changes in emotion, attention, learning, and action depend on neurons with a very different pattern of connectivity. Such neurons include midbrain dopamine neurons, which have cell bodies in the substantia nigra and ventral tegmental area of the midbrain, and highly divergent projections that connect with the frontal cortex, dorsal and ventral striatum, and other forebrain regions. Midbrain dopamine neurons go awry in Parkinson's disease, schizophrenia, and drug addiction. Data from both human and animal research implicate this small but widely connected neuronal population in motor control, motivation, effort, reward, analgesia, stress, learning, attention, and cognition. On page 1898 of this issue, Fiorillo *et al*. (*1*) report a new response mode for midbrain dopamine neurons and speculate how this new mode might contribute to the allure of gambling.

The authors are at the Center for Studies in Behavioral Neurobiology, Concordia University, Montréal, Quebec, H3G 1M8, Canada. E-mail: shizgal@csbn.concordia.ca; andreas@csbn.concordia.ca